Gao, F.; Calatayud Lorente, V.; García-Breijo, F.; Reig Armiñana, J.; Feng, Z. (2016). Effects of elevated ozone on physiological, anatomical and ultrastructural characteristics of four common urban tree species in China. Ecological Indicators. 67:367-379. doi:10.1016/j.ecolind.2016.03.012.

Effects of elevated ozone on physiological, anatomical and ultrastructural characteristics of four common urban tree species in China

Feng Gao[a,1], Vicent Calatayud[a,b,1], Francisco García-Breijo[c,d], José Reig-Armiñana[c], Zhaozhong Feng[a*]

[a]State Key Laboratory of Urban and Regional Ecology, Research Center for Eco-Environmental Sciences, Chinese Academy of Sciences, Shuangqing Road 18, Haidian District, Beijing 100085, China

[b]Fundación CEAM, c/Charles R. Darwin 14, Parque Tecnológico, 46980 Paterna, Valencia, Spain

[c]Laboratorio de Anatomía e Histología Vegetal ‘‘Julio Iranzo’’, Jardín Botánico, Universitat de València, c/Quart, 80, 46008 Valencia, Spain.

[d]Departamento de Ecosistemas Agroforestales. ETSIAMN. Universidad Politécnica de Valencia. Camino de Vera s/n, 46022-Valencia, Spain.

*Corresponding author: Zhaozhong Feng. E-mail: fzz@rcees.ac.cn, Tel: +86-10-62943823, Fax: +86-10-62943822;

[1]Both authors contributed equally to this work.

Abstract

Fast urbanization has led to ozone (O_3) being the main pollutant in summer in most of China. To assess future ground-level O_3 effects on the service of urban greening species and clarify the underlying mechanism of O_3 damage, four common urban greening species of *Ailanthus altissima* (AA), *Fraxinus chinensis* (FC), *Platanus orientalis* (PO) and *Robinia pseudoacacia* (RP) were exposed to non-filtered air (NF) and to elevated O_3 (E-O_3) in open-top chambers. E-O_3 induced visible injury in all species as well as microscopic alterations such as collapse of the palisade parenchyma cells, callose accumulation, or chloroplast and mitochondrial accelerated senescence. E-O_3 significantly reduced light-saturated CO_2 assimilation (A_{sat}), the maximum activity of Rubisco (Vc_{max}), the maximum electron transport rate (J_{max}), and fluorescence parameters such as the quantum yield of noncyclic electron transport (ϕ_{PSII}), and the quenching of photochemical efficiency of PSII (qP). It also increased total antioxidant capacity, phenolics and ascorbate contents. No significant interaction between O_3 and species was found in photosynthetic performance and antioxidant systems, suggesting that the four species selected were sensitive to O_3. Of all four species, AA was the most sensitive species due to a combination of earlier injury onset, anatomical features, lower antioxidant and higher stomatal conductance. The sensitivity of tree species to O_3 is a factor to be considered for urban greening. Ozone may affect important urban forest ecosystem services by reducing CO_2 assimilation.

Keywords

Antioxidant system, Ozone, Photosynthesis, Ultrastructure, Urban greening species

Capsule

Ground-level ozone negatively affects common greening tree species in China

Abbreviations

A = photosynthetic rate

AA = *Ailanthus altissima*

AOT40 = accumulated hourly O_3 concentration over a threshold of 40 ppb during daytime

AsA = ascorbate

A_{sat} = light-saturated photosynthesis

BVOC = biogenic volatile organic compounds

C_a = ambient CO_2 concentration

Car = carotenoid

Chl = chlorophyll

C_i = intercellular CO_2 concentration

F_v'/F_m' = actual photochemical efficiency of PSII in the saturated light

FC = *Fraxinus chinensis*

ϕ_{PSII} = the quantum yield of noncyclic electron transport.

g_s = stomatal conductance

J_{max} = the maximum rate of electron transport

LM = light microscopy

LMA = leaf mass per area

L_s = stomatal limitation to photosynthesis

O_3 = ozone

OTC = open-top chambers

PBS = phosphate buffered saline solution

PO = *Platanus orientalis*

RP = *Robinia pseudoacacia*

TEM = Transmission Electron Microscopy

qP = quenching of photochemical efficiency of PSII

Vc_{max} = the maximum carboxylation efficiency

WUE = water use efficiency

1. Introduction

Tropospheric ozone (O_3) levels are of great concern as this pollutant affects human health, ecosystem services and food security besides being a greenhouse gas (The Royal Society, 2008; IPCC, 2013). For sensitive plants, high O_3 concentration is known to induce visible injury, impair photosynthesis, produce reductions in growth and yield, and alter plant interactions with pests and diseases (Krupa et al., 2000).

Projected changes of the annual daily mean maximum eight-hour (DM8H) surface O_3 concentrations are expected to be in the range of 2 to 8 ppb, -3 to 8 ppb, and -7 to 9 ppb for the 2020s, the 2050s, and the 2090s in summertime for the whole East Asia (Lee et al., 2015). Ozone concentrations in China are rising at a higher rate than in other countries because O_3 precursors (mainly NO_2) have steadily increased at annual growth rate of 5% caused by its fast industrialization and urbanization (Wang and Mauzerall, 2004; Feng et al., 2015a). In Beijing, the monthly average of peak O_3 concentrations is currently 100 ppb in July, while the AOT40 (accumulated hourly O_3 concentration over a threshold of 40 ppb during daytime) from June to August is 29 ppm.h (Feng et al., 2015b; Yuan et al., 2015). The yearly average of O_3 concentration in Beijing cities reaches more than 60 ppb during May 2014 to April 2015 (Chen et al., 2015), and short-term projected emissions suggest that O_3 concentration will further increase (Yamaji et al. 2008). Therefore, current O_3 levels are, and future O_3 levels are expected to be by far above the threshold value of 40 ppb and AOT40 critical level of 5 ppm.h, which have been established to protect sensitive plants against O_3 (LRTAP, 2010).

Cities are characterized by higher levels of pollutant emissions, energy consumption and higher temperatures (heat island effect) than surrounding areas. One of the multiple environmental benefits of vegetation is the improvement in air quality (Nowak et al., 2014). In the central part of Beijing, the removal of pollutants by trees was quantified to be 1261.4 tons in 2002, mostly particles (61%), with O_3 accounting for 20% (Yang et al., 2005). However, biogenic volatile organic compounds (BVOCs) emitted from vegetation such as isoprene and monoterpenes are precursors of O_3 (The

Royal Society, 2008), so the contribution of urban trees to O_3 formation can even offset their removal capacity (Yang et al., 2005). Therefore, it is important to select plants with low BVOC emission rates, high pollutant removal capacity and also tolerant to air pollutants when planting trees in cities. The present paper focuses on the latter aspect.

In Beijing, O_3 concentrations are high enough to induce visible injury in sensitive species and cultivars, including several ornamental trees (Feng et al., 2014). These symptoms are observed in large gardens or urban forests in parks inside the city, or in crop areas or tree plantation surrounding the city rather than in streets where high NO traffic emissions locally scavenge O_3 (due to the titration effect). Ozone effect on plants depends both on the O_3 dose entering the plant through the stomata which is directly related to water vapor stomatal conductance (g_s), and also on their defense ability to cope with oxidative stress (Matyssek et al., 2007; Paoletti et al., 2008). On the other hand, leaf functional traits are considered to play a role in O_3 sensitivity, e.g. plants with higher leaf mass per area (LMA), or higher thickness or density of mesophyll tissues being tolerant to O_3 (Bussotti, 2008; Zhang et al., 2012).

However, information on the effects of current and predicted future O_3 levels on urban greening species is still very scarce in China. In the present study, we exposed four commonly planted urban greening tree species to elevated O_3 level which is the representative of a future scenario by 2050 on the basis of annual increase rate of 0.73 ppb/year at Shangdianzi station observation nearby Beijing city (Dr. XB Xu, personal communication) and an increase rate of 0.5-2% at a global scale (Vingarzan, 2004). The four species are the tree of heaven (*Ailanthus altissima* (Mill.) Swingle, AA), the Chinese ash (*Fraxinus chinensis* Roxb., FC), the American sycamore (*Platanus orientalis* L., PO) and the black locust (*Robinia pseudoacacia* L., RP) . Three of them (AA, FC, RP) are regarded as O_3 sensitive. This study tests the following two hypotheses: (1) O_3 sensitivity differs among investigated species, considering anatomical and ultrastructural changes, photosynthetic performance and antioxidant

systems; (2) plants with a higher stomatal conductance, lower antioxidant capacity and thinner leaves are more sensitive to O_3.

2. Materials and methods

2.1. Plant materials

One-year-old seedlings of AA, FC, PO and RP were obtained from a commercial nursery near the experimental site. Bare rooted seedlings were planted in 20 L circular plastic pots on 31 March 2013 and grown at ambient field condition. Pots were filled with native light loamy soil (pH 7.96, Organic C 14.7 g/kg; total N 1.64 g/kg, available P 6.59 mg/kg, available K 139.8 mg/kg) randomly selected from a nearby farmland. Plants with similar height and basal diameter were selected. Ten days before O_3 fumigation, they were pre-adapted to open-top chamber (OTC, octagonal base, 12.5 m^2 of growth space with a diameter of 4 m, and 3.0 m in height). All plants were watered at field capacity at 1-3 day intervals to avoid water stress. Solid, slow-release fertilizer (N/P/K = 17,17,17) was applied at a rate of 300 kg ha^{-1} to each plant at July during the experiment.

2.2. O_3 treatments

The experiment was carried out at Changping (40°19′N, 116°13′E), Northwest Beijing. The area has a semi-humid continental climate, with a yearly precipitation of 550 mm, and an annual mean temperature of 11.8 °C. Plants were exposed to two O_3 treatments in OTCs for four and a half months (from 1 June to 15 October): non-filtered ambient air (NF, averaged O_3 concentration of 42 ppb from 09:00 to 18:00), and NF supplied with 40 ppb of O_3 (E-O_3, averaged O_3 concentration of 69 ppb from 09:00 to 18:00). The four species and two O_3 treatments were selected for the present study from a wider investigation involving a total of 10 species and six different O_3 regimes in six OTCs. Positional effects were avoided by changing plant positions within each OTC weekly, and by switching them randomly among six OTCs monthly (Feng et al., 2011a). For each O_3 treatment, 4-6 plant replicates were used for

each species. Ozone was generated from pure oxygen using an O_3 generator (HY003, Chuangcheng Co., Jinan, China), mixed with ambient air and then piped into OTCs through a PVC tube (11 cm in diameter) using a fan (1.1 kW, 1080 Pa, 19 m^3 min^{-1}, CZR, Fengda, China). The flow rate of pure oxygen was regulated by mass flow controllers so as to achieve the target O_3 concentration at the top of the canopy in the fumigation treatments. An O_3 analyzer (Model 49i-Thermo, USA) was used to continuously monitor O_3 concentrations inside the OTCs via a Teflon solenoid valve switch system connected to a set of Teflon tubes (4 mm in diameter), which collected air from sampling points at approximately 10 cm above the plant canopy in each chamber. The monitors were calibrated by a 49i-PS calibrator (Thermo Scientific, USA) before the experiment and once a month during the experiment. The daily maximum fumigation period was 9 h (from 09:00 to 18:00) through a fan running when there was no rain, fog, mist, or dew, according to the protocols in free air O_3 concentration enrichment system (Feng et al., 2011b). The monthly ambient O_3 concentration (from 09:00 to 18:00) in the open field was ranged from 43 ppb (September) to 69 ppb (June), with the highest one hour peak being 153 ppb (at 16 h on 20 September) .

2.3. Visible injury

Visible injury was assessed weekly in all plants (4-6 per O_3 treatment). The percentage of injured leaves (for PO, with simple leaves) or leaflets (for the rest of species, with composite leaves) per plant was scored, in order to classify each plant according to the following classes: 0, no leaves injured; 1, ≤1% leaves injured; 2, >1% – ≤10% leaves injured; 3, >10% – ≤50% leaves injured; 4, >50% leaves injured.

2.4. Leaf traits

Twenty-five asymptomatic mature leaves from NF plants were collected studying the leaf traits using a scanner and ImageJ software (Gao et al., 2011). LMA was calculated as dry mass (mg) / leaf surface area (cm^2). Leaf dry mass was determined

193 by oven-drying leaves at 60 °C for 40 h until steady weight. To estimate the leaf traits,
194 paraffin-embedded sections of six leaves or leaflets (five sections per leaf or leaflet,
195 and five measurements made per section) were examined under the microscope
196 following the methods described below.
197
198 *2.5. Microscopy examinations*
199 To study the effects of O_3, six symptomatic and six asymptomatic leaves or leaflets
200 from the upper canopy layer (6-8th fully expanded leaves from the top) of three plants
201 for each species were collected in August from E-O_3 and NF plants, respectively,
202 before the onset of senescence. Samples were fixed in 2% Karnovsky fixative for 8 h
203 at 4°C, then washed three times for 15 min with 0.01 M PBS (pH 7.4). For
204 microscopy examinations, leaf portions were submitted to freeze-cut, paraffin- and
205 resin-embedded sections. For freeze-cut sections (~30 µm), a freezing microtome
206 (CM 1325; Leica, Germany) was used, paraffin-embedded sections (~10 µm) were
207 cut with an Anglia Scientific microtome, and Spurr's resin-embedded samplers were
208 cut with a diamond knife (DIATOME Histo 45°) and an ultramicrotome (Ultratome
209 Nova LKB Bromma) (~1.5 µm). Freeze-cut sections were observed under
210 epifluorescence BV (autofluorescence) or stained with aniline blue and observed
211 under epifluorescence UV to detect callose depositions. For fluorescence microscopy,
212 an Olympus U-ULS 100 HG epifluorescence system with U-MWU (excitation filter
213 330–385 nm, dichroic mirror 400 nm, barrier filter 420 nm) and U-MWBV (excitation
214 filter 400–440 nm, dichroic mirror 455 nm, barrier filter 475 nm) cubes was used.
215 Paraffin-embedded sections were stained with safranin-fast green, or with trichromic
216 FSA for observation of the different structures and for identifying their composition.
217 Semi-thin sections were stained with toluidine blue. Pectinaceous drops were detected
218 with this stain. All light microscope (LM) observations were carried out by an
219 Olympus Provis AX 70 fluorescence microscope equipped with an Infinity 2-3C
220 Lumenera® digital camera and analyzed with "Infinity Analyze" Software v.6.4.1.
221 For transmission electron microscopy (TEM), samples were fixed as LM, then

washed three times with 0.02 M PBS (pH 7.4) for 15 min and fixed again with 2% osmium tetroxide (OsO_4) in 0.01 M PBS (pH 7.4) for 2 h at room temperature. After washing in buffer, samples were dehydrated and embedded as indicated for LM. Ultrathin sections 80 nm thick were made with a diamond knife (mod. DIATOME ultra 458 ; DIATOME, Hatfield, PA, USA), mounted on copper grids of 100 mesh, and then stained with 10 % uranyl acetate and 0.1% lead citrate using the 'Synaptek Grid-Stick Kit' (EMS; http://www.ems-diasum.com/microscopy/technical/datasheet/71175.aspx). Sections were observed at 80 kV under the JEOL JEM-1010 microscope (JEOL USA Inc, Peabody, MA, USA). Images were obtained using an Olympus MegaView III camera and processed by Olympus analysis getIT software (Olympus Corp., Japan). In total, 40–50 root segments were examined through TEM.

2.6. Leaf gas exchange and chlorophyll a fluorescence measurements

Two upper canopy leaves (6-8th fully expanded leaves from the top) from each plant, i.e. eight leaves from four plants for each species, were selected randomly. Gas exchange and chlorophyll *a* fluorescence were determined simultaneously from 9:00 to 11:00 at both August and September using a LiCor-6400 photosynthesis system (LICOR, Lincoln, NE, USA) fitted with a 6400-40 leaf chamber fluorometer (LCF). During the measurements, photosynthetic active radiation (PAR) was set at 1200 μmol m^{-2} s^{-1}, CO_2 levels at 380 ppm, block temperature at 32 ± 0.5 °C and relative humidity between 50% and 70%. Fluorescence parameters include actual photochemical efficiency of PSII in the saturated light (F_v'/F_m'), quenching of photochemical efficiency of PSII (qP), and the quantum yield of noncyclic electron transport (ϕ_{PSII}). Water Use Efficiency (WUE) was calculated as the ratio between light-saturated photosyntehsis rate (A_{sat}) and transpiration rate.

During the experiment, photosynthesis and intercellular CO_2 concentration (A/*C*i) curves were performed in four plants (one leaf per plant, selected from the 6-8th fully expanded leaves from the top) for either O_3 treatment, using the automatic program in

the LiCor-6400 photosynthesis system. When the stomatal conductance (g_s) reached equilibrium, subsequent measurements were made following step-wise changes in reference CO_2 concentration: 380, 300, 200, 100, 50, 400, 600, 900, 1200, 1500 ppm, under PAR of 1200 μmol m^{-2} s^{-1}, block temperature of 32 ± 0.5 ˚C and relative humidity of 50-70%. The maximum carboxylation efficiency (Vc_{max}) and the maximum rate of electron transport (J_{max}) were derived by iteratively fitting curves to A/*C*i response data according to the program of Sharkey et al. (2007). Stomatal limitation (L_s) was calculated as $L_s = 1- A_{Ca380}/A_{Ci380}$, where A_{Ca380} and A_{Ci380} represent net CO_2 assimilation rate at ambient CO_2 concentration (*C*a) of 380 ppm and at *C*i = 380 ppm, respectively.

2.7 Pigment and antioxidant content

Those leaves (6-8th fully expanded leaves from the top) for photosynthesis measurements were used again for pigment and antioxidant assays in both NF and E-O_3 plants in September. Leaf discs (~10 mm diameter) in two leaves per plant were plunged from 4-5 plants of each species between 11:30 and 12:30, wrapped tinfoil, frozen in liquid nitrogen, and stored at -80℃ until physiological and biochemical analysis.

2.7.1. Pigments content

The pigment content of two leaf discs (~10 mm diameter) from two leaves per plant in either O_3 treatment was extracted with 4 ml 95% ethanol in the dark for 72 h at 4°C. The absorbance of leaf pigment extracts was measured at 646 nm, 663 nm and 470 nm. Total chlorophyll (Chl) and carotenoid (Car) contents were calculated according to the specific absorption coefficients provided by Lichtenthaler (1987).

2.7.2. Ascorbate (AsA) content

Two leaf discs from two leaves per plant (~30 mg) were homogenized in a pre-chilled mortar and extracted in 2 ml ice-cold 6% (w/v) trichloroacetic acid, and then

centrifugated at 13,000 *g* for 5 min at 4ºC. Reduced and total ascorbate (AsA) contents were determined following the protocol of Gillespie and Ainsworth (2007).

2.7.3. Total antioxidant capacity (TAC) and total phenolics content

For total antioxidant capacity (TAC), 2 ml cold 70% (v/v) ethanol was added to leaf disc samples (~ 30 mg) and homogenized in darkness. The mixture was centrifuged at 13,000 *g* for 10 min. Subsequently, 0.1 ml of supernatant was taken for the ferric reducing antioxidant power (FRAP) assay to express the total antioxidant activity. The principle of the assay was conducted following the method of Benzie and Strain (1996), expressed as Fe^{3+} equivalents (mmol Fe^{2+}/g fresh mass).

For phenolics content, 2 ml cold 95% (v/v) methanol was added to leaf disc samples (~ 30 mg). The mixture was incubated for 48 h in darkness, then centrifuged at 13,000 *g* for 10 min in darkness. 0.1 ml of supernatant was taken for total phenolics analysis, using Folin-Ciocalteau reagent as described by Ainsworth & Gillespie (2007), and expressed as mg of gallic acid equivalents per unit of fresh mass.

2.8. Statistical analyses

In this study, each plant was treated as the statistical unit, i.e. plant means were firstly obtained and statistical analyses were applied subsequently. In order to test the effects of O_3, species, sampling date and their interactions, the data of each dependent variable was subjected to the analysis of variance with a Mixed Lineal Model using JMP software (SAS Institute, USA). Except reduced ASC, TAC and *q*P with square root transformation, all variables in the original data passed the homogeneity test of variance. In case of significant interactions between O_3 and species, differences among species in combination with O_3 treatment were tested with an ANOVA followed by Tukey's HSD. Otherwise, Student *t*-test was applied to compare the difference between O_3 treatments for any variable at any sampling date. $P \leq 0.05$ was considered statistically significant. Data shown in Tables and Figures are means ± SE (n = 4-6, excluding Table 1 with n = 6-25).

3. Results

3.1. Leaf traits

Three species (AA, FC and RP) have composite leaves, and the other one (PO) has large single leaves. LMA was on average higher in AA and FC, and lower in PO and RP. AA was the species showing the smallest palisade parenchyma. Upper epidermis was thicker in AA and PO than in the other two species, and mesophyll thickness ranked as FC and PO > RP and AA (Table 1).

318 Table 1. Leaf traits of the four species. For AA, FC and RP with composite leaves,
319 measurements are based on leaflets. Different letter indicates significant difference
320 between species.
321

	Units	AA	FC	PO	RP
Length	cm	16.7 ± 0.3a	10.1 ± 0.2b	15.9 ± 0.7a	5.3 ± 0.1c
Width	cm	4.7 ± 0.1b	4.5 ± 0.1b	18.6 ± 1.4a	2.3 ± 0.0c
Perimeter	cm	38.1 ± 0.7b	23.3 ± 0.4c	82.0 ± 5.8a	12.6 ± 0.1d
Leaf area	cm^2	56.2 ± 1.8b	30.8 ± 1.1c	231.7 ± 21.4a	10.1 ± 0.2d
Leaf mass per area	mg cm^{-2}	9.1 ± 0.9a	8.8 ± 0.2a	5.6 ± 0.2b	5.0 ± 0.3b
Upper epidermis	μm	19.5 ± 0.2a	10.2 ± 0.2c	20.3 ± 0.6a	13.4 ± 0.4b
Lower epidermis	μm	10.1 ± 0.2b	10.4 ± 0.2b	15.0 ± 0.5a	11.3 ± 0.3b
Palisade parenchyma thickness	μm	49.0 ± 1.6c	68.5 ± 0.9a	71.2 ± 2.1a	60.8 ± 0.7b
Spongy parenchyma thickness	μm	49.9 ± 1.3b	72.7 ± 2.5a	68.4±1.9a	43.7 ± 1.2b
Mesophyll thickness	μm	99.0 ± 2.7b	141.3 ± 3.2a	139.6 ± 3.6a	104.4 ± 1.2b

322
323 *3.2. Visible injury*
324 No visible injury was observed in any of the plants in NF treatment (control). The
325 onset of O_3 symptoms in E-O_3 was at the following dates: AA at 04/07/2013, PO at
326 11/07/2013, RP at 18/07/2013 and FC at 06/08/2013, and the corresponding AOT40
327 values were 12.8, 14.2, 16.2, 23.2 ppm. h, respectively. From Fig. 1, AA was the
328 species showing symptoms earliest, and was also the most severely affected from the
329 beginning, although towards the end of the experiment the percentage of injured
330 leaves was reduced due to the development of new, not injured leaves. Photos of
331 E-O_3-induced visible injury are provided in Fig. 2.
332

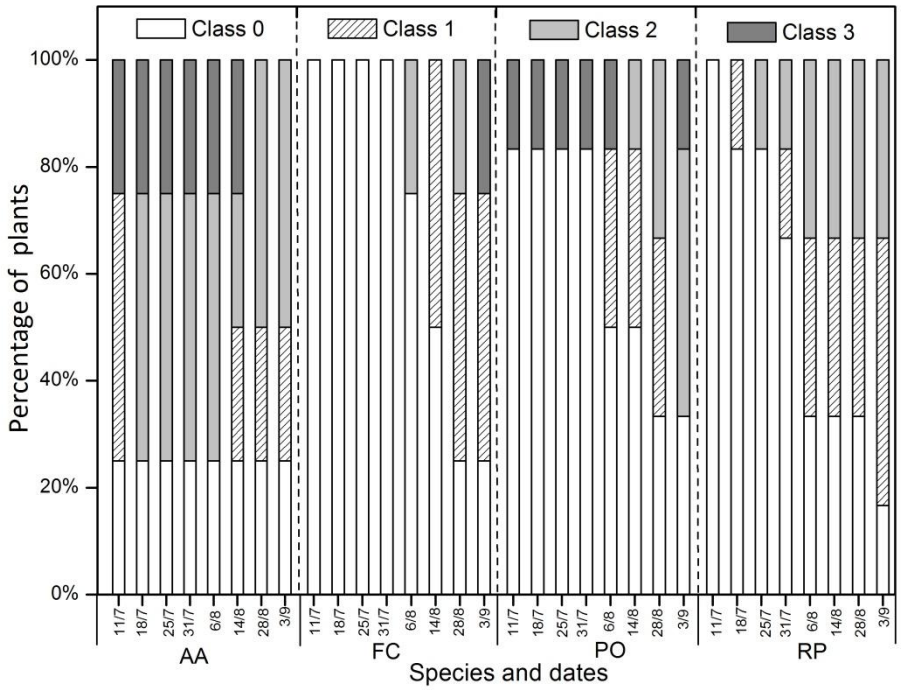

333

334 **Figure 1**. Percentage of plants belonging to different classes. Classes: 0, no leaves
335 injured; 1, ≤1% leaves injured; 2, >1% – ≤10% leaves injured; 3, >10% – ≤50%
336 leaves injured.

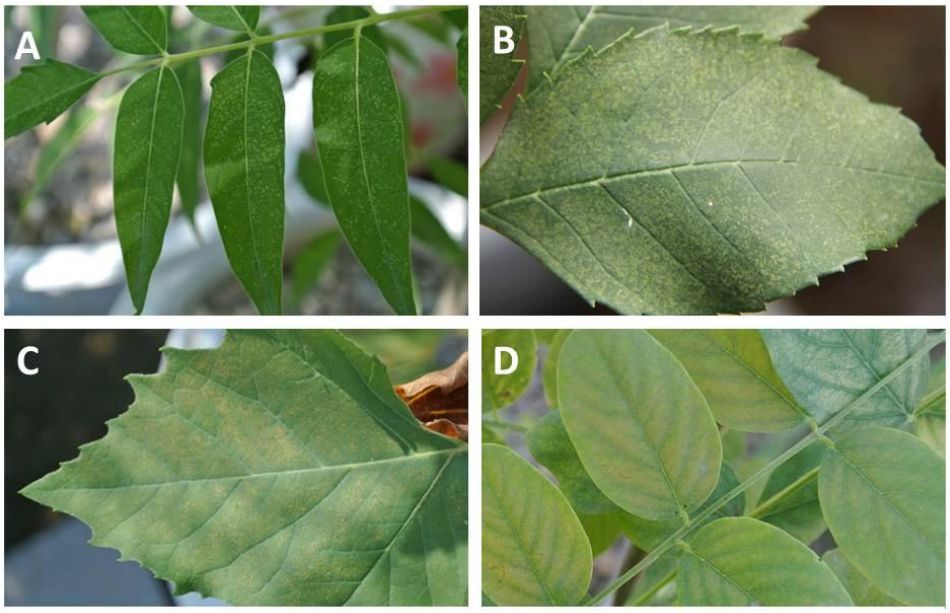

337

338 **Figure 2**. Visible symptoms in (**A**) *Ailanthus altissima*. (**B**) *Fraxinus chinensis*. (**C**)
339 *Platanus orientalis*. **(D)** *Robinia pseudoacacia.*

340

341 *3.3 Anatomical and ultrastructural changes induced by E-O_3*

342 LM and TEM studies showed the effects of O_3 as well as plant responses against
343 oxidative stress. Palisade parenchyma cells were in general the most affected part of
344 the mesophyll (AA > PO > FC > RP; see Fig. 3). The middle lamella of the cell wall
345 was degraded (Figs 4A, 5B) and small pectinaceous drops produced by its
346 degradation were observed (Figs. 4A, 5A, 5E, 5F, 6A). Cell walls were progressively
347 altered (Figs. 3C,3F, 4B, 4C, 5B, 5C, 7C, 7E), and fluorescence LM (Fig. 3A) and
348 TEM (Figs. 5A, 5B, 6B) showed that callose was accumulated between the membrane
349 and cell wall, especially in AA and PO. Inside the cells, vacuole content becomes
350 altered. In AA and RP, vacuolar content of the affected cells became denser by the
351 accumulation of tannins (Figs. 3B, 3H), and in PO, the normal cells of which have
352 vacuoles with abundant tannic content, a gradual coagulation of tannins in the
353 affected cells was observed (Figs. 5E, 5F), as well as a large accumulations of crystals
354 in their cytoplasm (Figs. 5D, 5D, 6C). Finally, tonoplast broke and cells lost turgor
355 (Fig. 7B). In a later stage, cells collapsed (Figs. 3, 4A, 4C, 5B, 5E, 5F, 7E) leading to
356 an increase of intercellular spaces (AA, PO > FC > RP). Chloroplasts were also
357 strongly affected in all species, increasing electrodense material and changing their
358 shape. Accumulation of big starch grains (Figs. 4A, 5B, 5C, 7A), abundant
359 plastoglobuli (Figs. 4A, 7A, 7B, 7C, 7E), and lipid-protein bodies (especially in AA,
360 Figs. 4A, 4B, 4D) were also observed. Finally, thylakoid membranes were partly or
361 totally disaggregated (Fig. 7B). Mitochondria also experienced degradation processes.
362 In some cases, the accumulation of lipid droplets similar to plastoglobuli was
363 observed, especially in AA (Fig. 4D). Similar but much less conspicuous changes
364 were observed in the spongy parenchyma. Upper and lower epidermises were not
365 distinctly affected in any of the species with an exception of AA and RP, in which
366 some epidermal cells can collapse (Figs. 3A, 3G, 4C). In some cases, chloroplast of
367 the guard cells of stomata were also affected, as indicated by large starch
368 accumulations (Fig. 7A). In the vascular bundles, xylem was never affected but

phloem cells can experience changes in shape and callose deposition may increase in the sieve tubes (Figs. 3H, 6E, 7D).

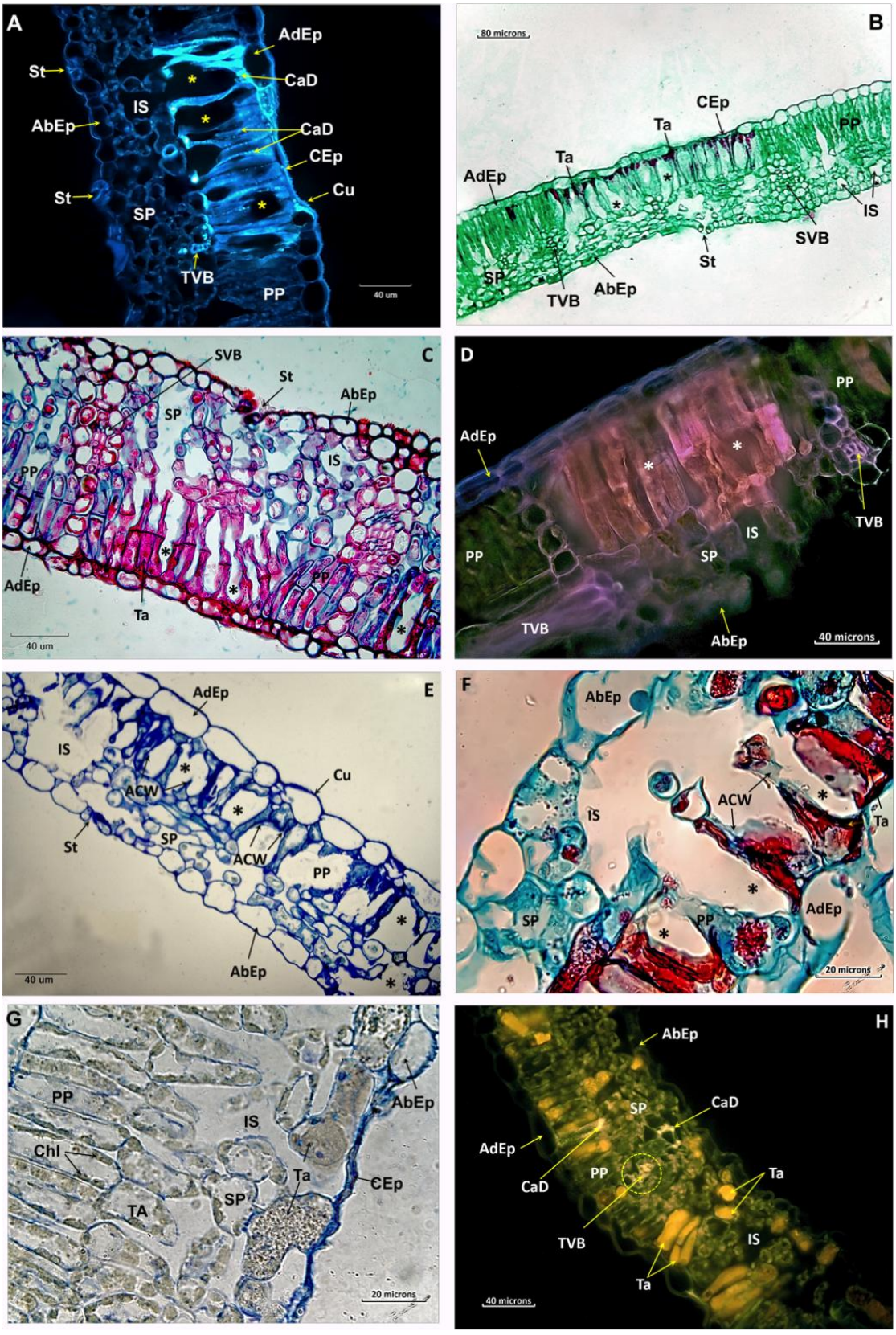

Figure 3. (**A**) Fluorescence micrograph (UV) of a cross section of *Ailanthus*

altissima leaf stained with aniline blue showing an affected area (**asterisks**) with numerous collapsed cells and with callose depositions (**CaD**) on its cell walls. **(B)** Micrograph of a cross section of an *Ailanthus altissima* affected leaf stained with safranin-fast green showing numerous collapsed cells (**asterisks**) with tannic (**Ta**) contents inside. **(C)** Micrograph of a cross section of a *Fraxinus chinesis* affected leaf stained with trichromic FSA showing numerous collapsed cells (**asterisks**) with tannic (**Ta**) contents inside. **(D)** Autofluorescence micrograph (BV) of a cross section of *Fraxinus chinensis* leaf showing an affected area (**asterisks**) of palisade parenchyma (**PP**) without chlorophylls. **(E)** Micrograph of a semithin cross section of a *Platanus orientalis* affected leaf stained with toluidine blue. Numerous collapsed cells (**asterisks**) leaving between them large intercellular spaces (**IS**) are observed. **(F)** Micrograph of a cross section of a *Platanus orientalis* affected leaf stained with trichromic FSA showing collapsed cells (**asterisks**) with affected cell wall (**ACW**) and tannic (**Ta**) contents inside. (G) Micrograph of a semithin cross section of a *Robinia pseudoacacia* affected leaf stained with toluidine blue. A collapsed epidermis (**CEp**) is observed. **(H)** Autofluorescence micrograph (BV) of a cross section of a *Robinia pseudoacacia* affected leaf. Numerous cells filled with tannin content (**Ta**) are observed. Others abbreviations. **AbEp**: abaxial epidermis; **AdEp**: Adaxial epidermis; **Cu**: cuticle; **TVB**: tertiary vascular bundle; **SP**: spongy parenchyma; **St**: stomata; **SVB**: secondary vascular bundle.

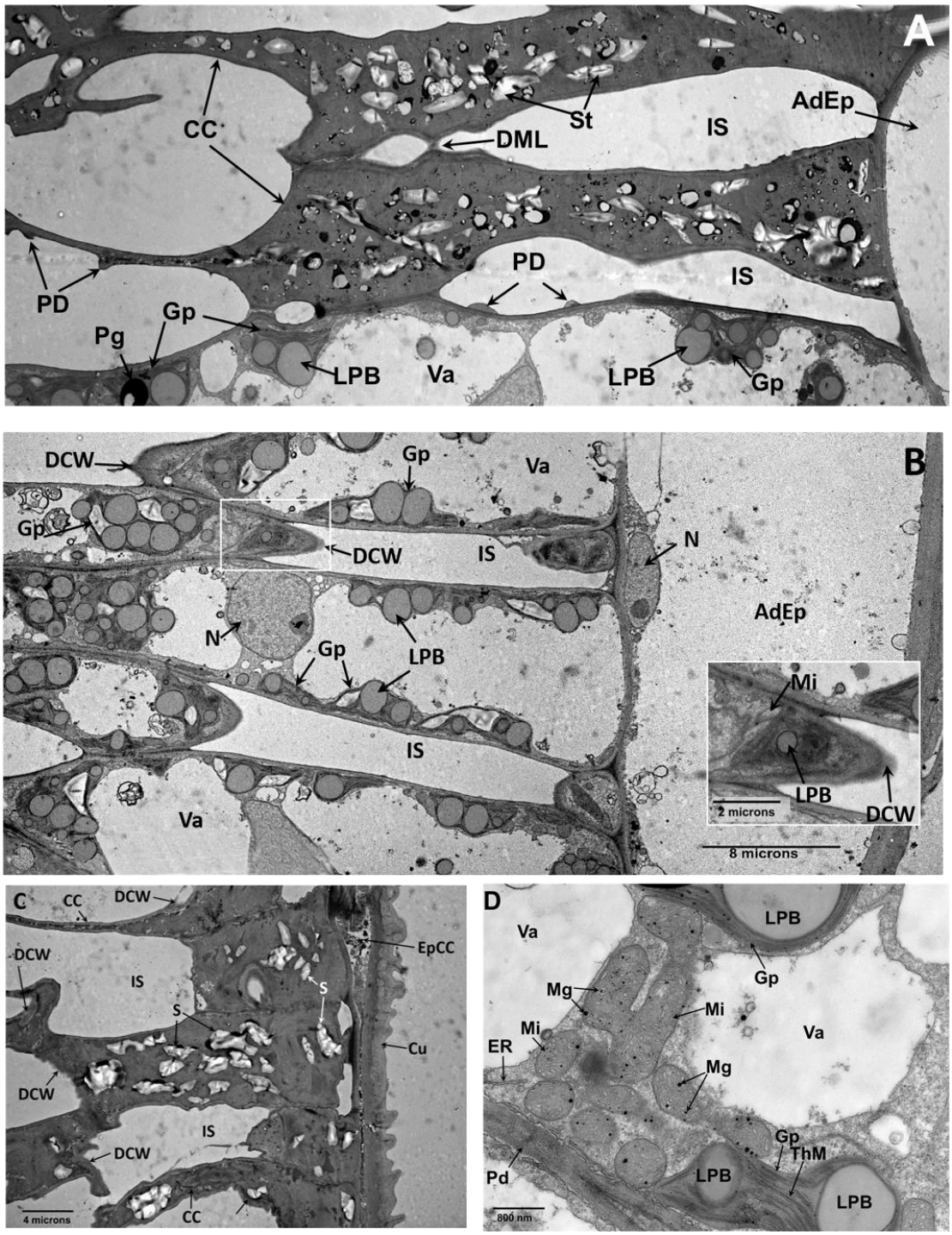

Figure 4. Details of TEM micrographs of cross sections of *Ailanthus altissima* leaves. **(A)** Two collapsed cells (**CC**) of palisade parenchyma with great intercellular spaces (**IS**). Pectinacious drops (**PD**) and degraded middle lamella (**DML**) are observed. **(B)** Cells of palisade parenchyma with abundant gerontoplasts (**Gp**) filled with abundant lipid-protein bodies (**LPB**), degraded cell wall (**DCW**) and great intercellular spaces (**IS**). The area marked with a white frame is shown magnified at

the bottom right of the image. **(C)** Collapsed cells (**CC**) of palisade parenchyma and adaxial epidermis (**EpCC**) showing a degraded cell wall (**DCW**). **(D)** Detail of a cell with several mitochondria (**Mi**) containing some mitoglobuli (**Mg**). Other abbreviations. **AdEp**: adaxial epidermis; **N**: nucleus; **Pd**: plasmodesma; **Pg**: plastoglobuli; **St**: starch; **ThM**: thylakoidal membranes; **Va**: Vacuole.

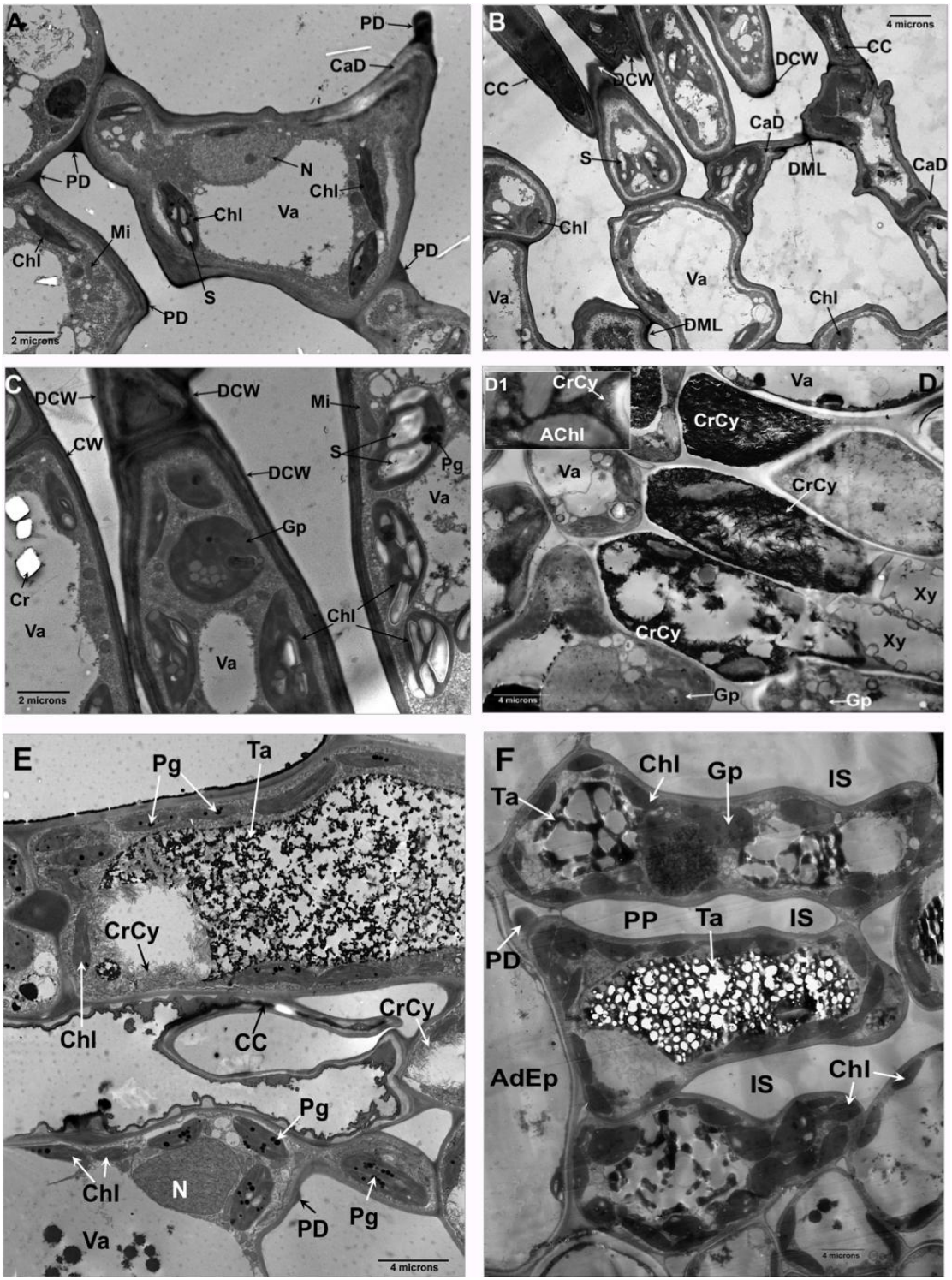

Figure 5. A to B: Details of TEM micrographs of cross sections of *Fraxinus chinensis* leaves. **D to F:** Details of TEM micrographs of cross sections of *Platanus orientalis* leaves. **(A)** Spongy parenchyma cell showing an altered medium lamella. Some pertinacious drops (**PD**) and callose depositions (**CaD**) between the cell membrane and cell wall are observed. **(B)** Cells of spongy and palisade parenchyma showing different alterations. Some of them are collapsed (**CC**). **(C)** Detail of palisade parenchyma cells. Degraded cell wall (**DCW**) and gerontoplasts (**Gp**) are observed. **(D)** Cells showing a crystalized cytoplasm (**CrCy**). In **(D1)** a detail of this crystallization is observed. **(E)** Affected palisade parenchyma cells. Collapsed cells (**CC**), vacuoles with tannins (**Ta**), crystalized cytoplasm (**CrCy**) and numerous chloroplasts (**Chl**) with plastoglobuli (**Pg**) are observed. (F) Cells of palisade parenchyma showing varying degrees of decomposition of tannins (**Ta**) within the vacuoles (**Va**). Other abbreviations. **AChl**: Altered chloroplast; **AdEp**: adaxial epidermis; **Cr**: (calcium oxalate) crystal; **DML**: degraded medium lamella; **N**: nucleus; **S**: starch; **Xy**: xylem.

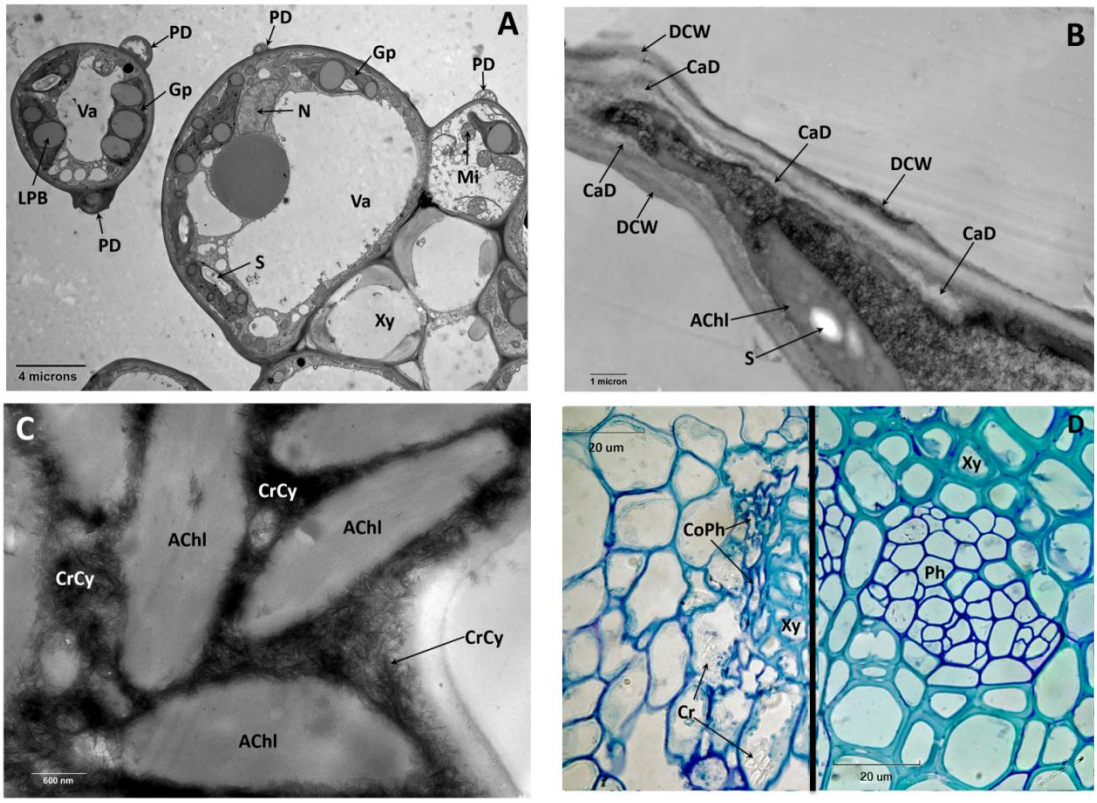

Figure 6. (**A)**. TEM micrograph of cross sections of *Platanus orientalis* leaf. Detail of spongy parenchyma cells showing pertinacious drops (**PD**). (**B).** TEM micrograph of cross sections of *Platanus orientalis* leaf. Callose depositions (**CaD**) between the cell membrane and cell wall are observed. (**C).** TEM micrograph of cross sections of *Platanus orientalis* leaf. Cell showing a crystalized cytoplasm (**CrCy**). (**D)**. Micrograph of a cross section of a *Fraxinus chinesis* affected leaf (left) and a control leaf (right) stained with toluidine blue. The affected leaf shows a collapsed phloem (**CoPh**). Other abbreviations. **AChl**: altered chloroplast; **Cr**: crystals; **CrCy**: crystalized cytoplasm; **DCW**: degraded cell wall; **Gp**: gerontoplast; **LPB**: lipid-protein body; **Mi**: mitochondria; **N**: nucleus; **Ph**: Phloem; **S**: starch **Va**: Vacuole; **Xy**: xylem.

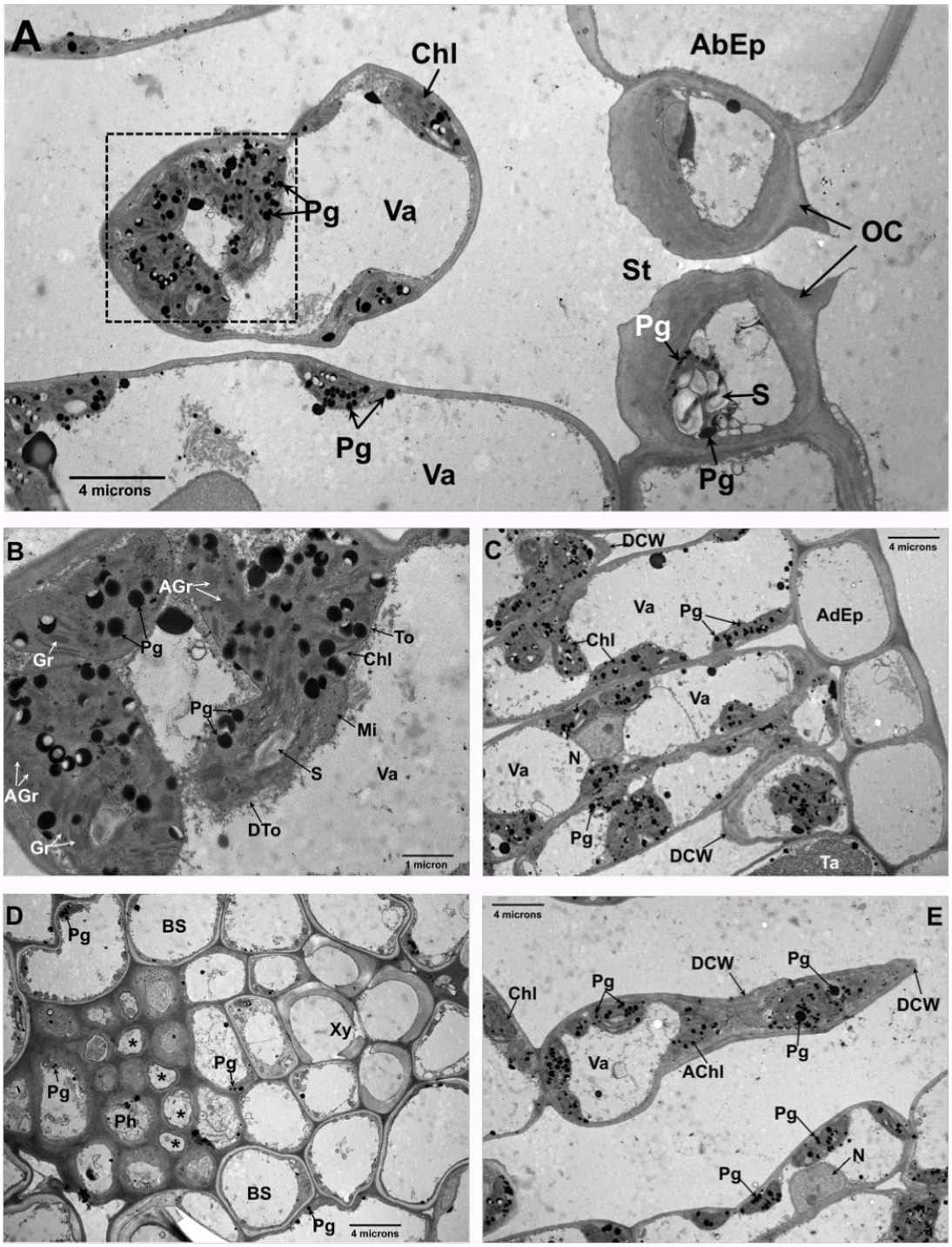

Figure 7. Details of TEM micrographs of cross sections of *Robinia pseudoacacia* leaves. **(A)** Detail of a stoma (**ST**) with affected chloroplast and spongy parenchyma. Chloroplast (**Chl**) in cells of spongy parenchyma are affected and contain numerous plastoglobuli (**Pg**). The area marked with the dashed square is shown in Figure (B). **(B)** Detail of affected chloroplasts containing numerous plastoglobuli and many grana disorganized (**AGr**). The tonoplast (**To**) is disintegrated into many areas (**DTo**). **(C)**

Palisade parenchyma cells containing chloroplasts with numerous plastoglobuli and degraded cell walls (**DCW**) in some areas. **(D)** Detail of a tertiary vascular bundle with the affected phloem. Callose depositions (**asterisks**) are observed in some phloem (**Ph**) vessels. **(E)** Cells affected in the spongy parenchyma. Their cell walls are degraded (**DCW**) and contain chloroplasts with numerous plastoglobuli (**Pg**). Other abbreviations. **AbEp**: abaxial epidermis; **AdEp**: Adaxial epidermis; **BS**: Bundle sheath; **Gr**: grana; **Mi**: mitochondria; **N**: nucleus; **OC**: occlusive cells; **S**: starch; **Ta**: tannins; **Va**: vacuole; **Xy**: xylem.

3.4. Leaf gas exchange and chlorophyll a fluorescence

Effects of E-O_3 on gas exchange and fluorescence parameters were significant for A_{sat}, ϕ_{PSII}, and qP (Table 2). There were no significant interactions between species and O_3, suggesting the responses to E-O_3 were the same among all species (Table 2). Effects on A_{sat} increased with O_3 exposure, as indicated that there was a significant reduction in A_{sat} by 27%, 21%, 17%, and 31% for AA, FC, PO and RP, respectively, in September (Tables 2 and 3). For the same month ϕ_{PSII} was significantly reduced by 13% and 21% in PO and RP, respectively (Table 3). C_i and WUE were not significantly affected by O_3, while g_s was significantly reduced in AA and RP in September. Notably, there was significant difference among species in g_s (Table 2), as shown by highest g_s values in AA (0.15 mol m^{-2} s^{-1}) and lowest in RP (0.07 mol m^{-2} s^{-1}), with FC and PO showing intermediate values (0.13 mol m^{-2} s^{-1}).

Table 2. Analysis of variance of the effects of O_3, species and sampling date, and their interactions on gas exchange and chlorophyll *a* fluorescence parameters, pigment and antioxidant contents.

	O_3	Species	O_3×Species	Date	O_3×Date	O_3×Date ×Species
A_{sat}	0.0002	<0.0001	0.9983	0.2049	0.0096	0.8472
g_s	0.5411	0.0002	0.5788	0.8176	0.0096	0.2809
C_i	0.7889	<0.0001	0.2548	0.7265	0.3888	0.3006
WUE	0.9437	0.1959	0.5503	<0.0001	0.3258	0.3105
*F*v'/*F*m'	0.6297	0.0002	0.0773	0.1689	0.3076	0.8374
ϕPSII	0.0427	<0.0001	0.5481	<0.0001	0.4844	0.7984
*q*P	0.0033	0.0065	0.6313	<0.0001	0.7380	0.3661
Vc_{max}	<0.0001	0.4209	0.5318	0.0337	0.8005	0.2668
J_{max}	<0.0001	0.0896	0.3419	0.1311	0.9928	0.3479
L_s	0.0006	0.2542	0.4295	0.2473	0.0148	0.9018
TAC	<0.0001	<0.0001	0.0965			
Phenolics	<0.0001	<0.0001	0.7386			
Total AsA	<0.0001	<0.0001	0.0908			
Reduced AsA	<0.0001	<0.0001	0.0799			
Chl a	0.0825	0.0991	0.8684			
Chl b	0.081	0.0403	0.9558			
Chl a+b	0.0815	0.0822	0.891			
Car	0.0715	0.0183	0.7867			
Chla/Chlb	0.2442	0.0200	0.816			

469 **Table 3**. Gas exchange and chlorophyll *a* fluorescence variables in plants grown in non-filtered air (NF) and in elevated O_3 (E-O_3) treatments in
470 August and September. Different letter indicates significant difference between O_3 treatments.
471

			A_{sat} (µmol m^{-2} s^{-1})	g_s (mol m^{-2} s^{-1})	C_i (ppm)	WUE (µmol CO_2 /mmol H_2O)	F_v'/F_m'	ϕ_{PSII}	qP
Aug.	AA	NF	11.33 ± 1.28	0.14 ± 0.03	236.32 ± 15.13	3.79 ± 0.33	0.38 ± 0.03	0.22 ± 0.03	0.56 ± 0.03
		E-O_3	11.33 ± 1.05	0.23 ± 0.07	276.32 ± 27.95	2.84 ± 0.62	0.46 ± 0.01	0.22 ± 0.02	0.47 ± 0.05
	FC	NF	12.79 ± 1.30	0.12 ± 0.02	205.87 ± 13.83	3.60 ± 0.26	0.44 ± 0.01	0.28 ± 0.01	0.62 ± 0.01
		E-O_3	12.07 ± 0.61	0.12 ± 0.02	206.27 ± 22.41	3.86 ± 0.47	0.46 ± 0.04	0.24 ± 0.02	0.53 ± 0.05
	PO	NF	8.91 ± 0.82	0.11 ± 0.01	242.29 ± 22.64	3.67 ± 0.55	0.45 ± 0.01	0.22 ± 0.00	0.48 ± 0.02
		E-O_3	7.98 ± 0.89	0.14 ± 0.02	284.54 ± 19.85	2.56 ± 0.50	0.45 ± 0.02	0.22 ± 0.02	0.49 ± 0.04
	RP	NF	7.99 ± 0.52	0.08 ± 0.01	214.51 ± 7.13	3.34 ± 0.18	0.36 ± 0.02	0.19 ± 0.01	0.52 ± 0.02
		E-O_3	7.53 ± 1.27	0.06 ± 0.02	156.39 ± 39.80	4.22 ± 0.71	0.37 ± 0.02	0.18 ± 0.03	0.48 ± 0.06
Sep.	AA	NF	12.47 ± 0.58a	0.15 ± 0.02a	236.36 ± 14.53	6.11 ± 0.79	0.40 ± 0.02	0.14 ± 0.01	0.36 ± 0.01
		E-O_3	9.14 ± 0.08b	0.09 ± 0.01b	221.73 ± 16.98	6.35 ± 0.71	0.48 ± 0.08	0.14 ± 0.00	0.33 ± 0.02
	FC	NF	13.32 ± 0.77a	0.17 ± 0.02	252.58 ± 14.25	5.54 ± 0.28	0.50 ± 0.03	0.20 ± 0.01	0.40 ± 0.01

	E-O_3	10.54 ± 0.65b	0.12 ± 0.01	244.34 ± 13.96	5.96 ± 0.33	0.44 ± 0.02	0.17 ± 0.01	0.40 ± 0.03
PO	NF	12.38 ± 0.10a	0.16 ± 0.01	258.47 ± 4.21	4.92 ± 0.23	0.51 ± 0.05	0.17 ± 0.00a	0.35 ± 0.03
	E-O_3	10.23 ± 0.18b	0.13 ± 0.02	249.55 ± 17.47	5.36 ± 0.45	0.46 ± 0.01	0.14 ± 0.00b	0.32 ± 0.01
RP	NF	9.55 ± 0.10a	0.09 ± 0.01a	172.74 ± 18.89	5.79 ± 0.52	0.38 ± 0.00	0.17 ± 0.00a	0.44 ± 0.01
	E-O_3	6.61 ± 0.09b	0.06 ± 0.01b	157.95 ± 17.30	5.76 ± 0.60	0.38 ± 0.03	0.13 ± 0.01b	0.36 ± 0.03

472

Ozone also induced significant reductions in carboxylation parameters across two measurements and four species (Table 2) , but for the gas exchange and fluorescence parameters, responses were similar between species as there were no significant interactions between species and O_3 (Table 2). In August, Vc_{max} was significantly reduced by 32% in PO and in September by 42% and 37% in AA and RP, respectively. J_{max} was reduced by 27% and 36% in FC and PO in August, and by 19% for FC in September (Fig. 8). E-O_3 also significantly reduced the stomatal limitation (L_s), which increased significantly with time (Table 2): reductions were significant for PO by 20% in August, for AA, FC and PO by 48%, 43% and 59%, respectively, in September (Fig. 8). No significant difference between species was found in carboxylation parameters and L_s.

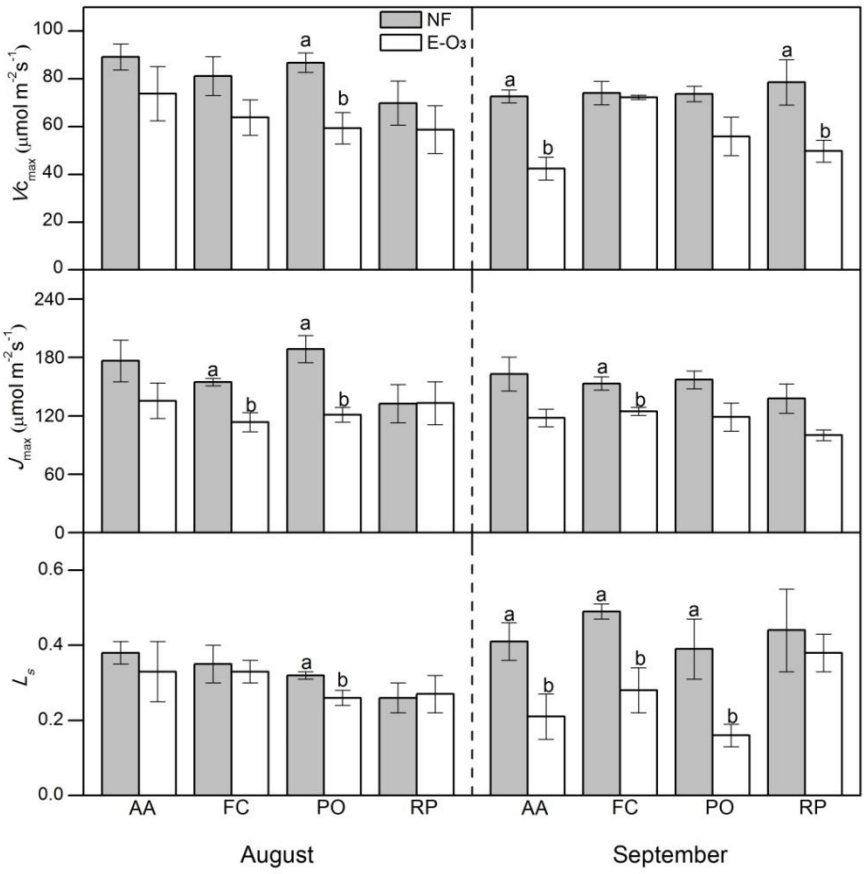

Figure 8. Carboxylation-related variables in plants grown in non-filtered air (NF) and

in elevated O_3 (E-O_3) treatment in August and September. Different letter indicates significant difference between O_3 treatments.

3.5. Pigment contents

Chlorophyll *b* (Chl *b*) and carotenoid (Car) contents as well as the Chl *a* / Chl *b* ratio differed significantly between species (Table 2) , as indicated by the highest Chl *b* and Car in FC and the lowest in PO, but both of them did not have significant difference from AA and RP (Table 4). Although mean values in chlorophyll and carotenoid contents were always lower in the E-O_3 treatment, these changes were not statistically significant at the measuring time (Tables 2 and 4).

Table 4. The Chlorophyll (Chl) and carotenoid (Car) contents in plants grown in non-filtered air (NF) and in elevated O_3 (E-O_3) treatments in September.

		Chl*a* (x10 mg m^{-2})	Chl*b* (x10 mg m^{-2})	Chl*a+b* (x10 mg m^{-2})	Car (x10 mg m^{-2})	Chl*a*/Chl*b*
AA	NF	17.98 ± 1.89	4.46 ± 0.37	22.43 ± 2.26	8.67 ± 0.59	4.02 ± 0.11
	E-O_3	13.23 ± 2.16	3.31 ± 0.55	16.54 ± 2.71	6.46 ± 0.98	4.00 ± 0.06
FC	NF	19.84 ± 2.09	5.52 ± 0.64	25.36 ± 2.72	9.72 ± 0.83	3.62 ± 0.07
	E-O_3	18.69 ± 3.29	5.05 ± 0.97	23.73 ± 4.26	9.12 ± 1.23	3.76 ± 0.11
PO	NF	14.61 ± 1.07	3.81 ± 0.27	18.42 ± 1.32	6.72 ± 0.52	3.84 ± 0.10
	E-O_3	12.63 ± 1.42	3.17 ± 0.38	15.80 ± 1.79	6.12 ± 0.59	4.00 ± 0.08
RP	NF	17.51 ± 2.97	4.49 ± 0.82	22.00 ± 3.79	8.10 ± 1.18	3.94 ± 0.05
	E-O_3	14.39 ± 1.75	3.65 ± 0.53	18.05 ± 2.28	6.88 ± 0.81	4.00 ± 0.15

3.6. Antioxidants

At the end of the growing season, plants in E-O_3 significantly increased their contents in antioxidant compounds (TAC, phenolics, total and reduced AsA) with regard to control plants (Table 2). Responses of different species to O_3 were similar for all tested antioxidant variables as indicated by no significant interaction (Table 2). Across

505 O_3 treatments, there was significant difference between species in TAC, phenolics and
506 reduce AsA contents (Table 2). Of all, PO had the largest antioxidant capacity, RP was
507 the lowest, and FC and AA ranked in the middle level. RP was the species with lower
508 constitutive levels of antioxidants, but it showed the strongest responses to O_3, with
509 increases of 67% in TAC, 67% in total phenolics, 85% in total AsA, and 65% in
510 reduced AsA in E-O_3 plants (Fig. 9). On the contrary, AA did not experience
511 significant changes in TAC and in reduced AsA after O_3 exposure (Fig. 9).

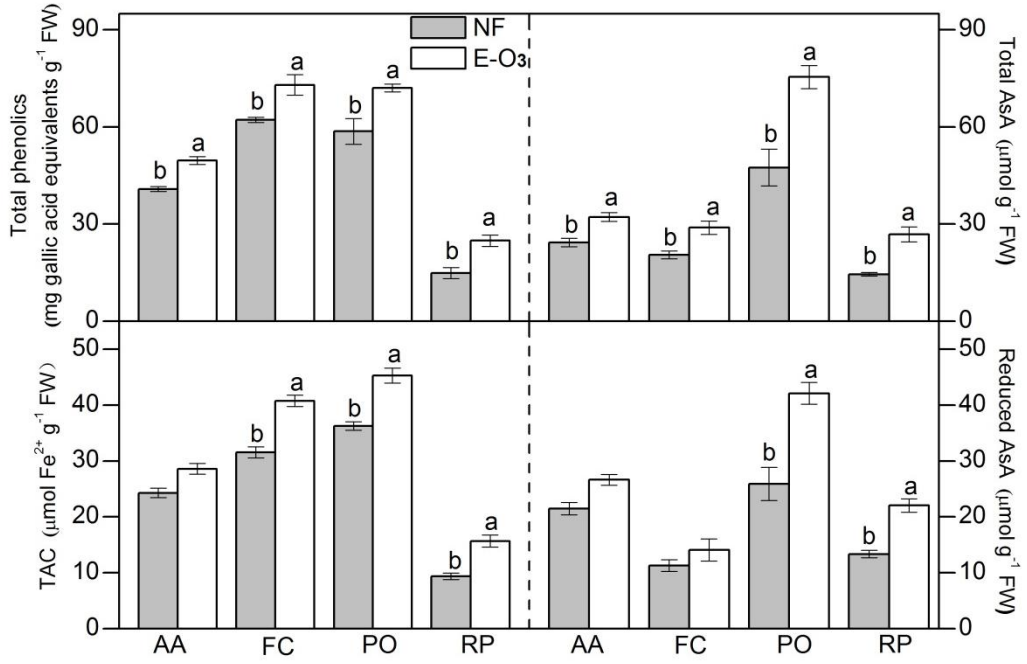

512

513 **Figure 9**. Total phenolics, total antioxidant capacity (TAC), total and reduced ascorbic
514 acid (AsA) contents in plants grown in non-filtered air (NF) and in elevated O_3 (E-O_3)
515 treatments in September. Different letter indicates significant difference between O_3
516 treatments.

517

518 **4. Discussion**

519 E-O_3 induced visible injury in the four investigated species with more severe effects
520 on AA, as 75% of the plants were affected before middle July. AA, FC and RP were
521 among the tree species showing symptoms in the field (Feng et al., 2014). AA can be
522 considered a good bio-indicator tree in Beijing area, because it was the tree species

showing symptoms at more sites and the symptoms were observed already in July with AOT40 of 12.8 ppm.h. Symptoms of these 3 tree species in E-O_3 were consistent with those observed in the field, supporting the validation of field observations in Beijing area.

Many of the anatomical and ultrastructural changes induced by E-O_3 are hypersensitive-like response (HR), in which oxidative burst (OB) plays a central role (Rao et al., 2000). Both are considered to be plant defence reactions against O_3 as well as other biotic and abiotic stresses (Sanderman et al., 1998; Vollenweider et al, 2003). OB triggers programmed death, leading to a cell collapse as observed in stippling areas in AA and PO. As shown in the present study, palisade parenchyma is usually the most affected tissue by O_3 (Günthardt and Vollenweider, 2007; Paoletti et al., 2009). Our observations suggest that reactive oxygen species (ROS) degrades the pectins of the middle lamella inducing a separation of the mesophyll cells, and increasing intercellular spaces. Hydrogen bounds between cellulose molecules and other cell wall components may also be affected, finally softening the cell which becomes deformed. Pectinaceous and polysaccharidic extrusions also result from the breakdown of the middle lamella. These projections have been reported in several species exposed to O_3 in fumigation chambers or in the field (e.g., Calatayud et al., 2011; Vollenweider et al., 2003), but are not specific of O_3 as they can be induced by other stress factors such as e.g. heavy metals (Günthard-Goerg and Vollenweider, 2007). Progressive degradation of the cell walls combined with the loss of turgor finally leads to cell collapse.

Callose accumulation is a defence response to abiotic and biotic factors such as wounding, desiccation, metal toxicity or insect attacks, and it has been postulated that it might act as a physical barrier against microbial and fungal attack (Stone and Clarke, 1992), isolating affected tissues from healthy cells. Ozone is considered to be an abiotic elicitor inducing responses similar to plant defence responses to pathogen attacks (Sandermann et al., 1998). Callose accumulation after O_3 exposure has been reported in different species (Gravano et al., 2003; Bussotti et al., 2005; García-Breijo

et al., 2008; Calatayud et al., 2011). Phenolic metabolites are suggested to play a protective role against oxidative stress as antioxidants (Kangasjärvi et al., 1994). In the four species, E-O_3 increased accumulation of phenolic compounds. In the vacuoles of AA and PO, rich in condensed tannins, these compounds changed their even distribution by a coagulated aspect most likely due to oxidative processes (Vollenweider et al., 2003). Changes in vacuole tannins due to O_3 have been observed in the mastic plant (Reig-Armiñana et al. 2004). In RP, less rich in tannins, an accumulation of phenolic compounds is observed. Previous microscopy studies have shown that accumulation of phenolic compounds including tannins and anthocyanins can be induced by O_3 in some species (Vollenweider et al., 2003; Bussotti et al., 2005).

At the ultrastructural level, changes in organelles that may be considered as an acceleration of the natural foliar senescence process can be observed. Foliar senescence is characterized by a decline in whole leaf gas exchange and protein levels, leaf yellowing, and the chloroplast-to-gerontoplast transition. Ultrastructurally, gerontoplast development is seen primarily as a progressive unstacking of grana, a loss of thylakoid membranes and a massive accumulation of plastoglobuli and other lipid-protein inclusions (Harris & Schaefer, 1981). In our study, ultrastructural changes in the chloroplast included an increase in electrodense material, accumulation of starch, plastoglobuli and lipid-protein bodies, thylakoid degradation, membrane disruption and changes in shape. Starch accumulation may be related to a difficulty in sucrose transport outside the chloroplasts and to other tissues (Calatayud et al., 2011). Landolt et al. (1997) found enhanced content of soluble sugars in leaves of O_3-exposed birch plants, and in the same species, Matyssek et al. (1992) observed accumulation of starch along veins, which suggested a reduction of carbon export from source leaves. This can be related with altered cell membranes and impaired phloem loading induced by O_3 (Grantz, 2003). In O_3-injured leaves, phloem cells can experience evident changes in shape, which may obviously impair their functionality and affect sucrose translocation (Calatayud et al., 2011). On the other hand, an

581 increase in plastoglobuli can originate from the lipid-soluble degradation products
582 from the thylakoid membranes (Matile, 1992; Kivimäenpää et al., 2010). Overall, the
583 four species show partly similar anatomical and ultrastructural changes that are
584 related both to O_3 damage to different cell components, defence responses and
585 accelerated senescence. Notably, changes were more evident in AA, with many
586 palisade parenchyma cells collapsed leading to a large intercellular spaces, distinct
587 callose dipositions, denser vacuolar content due to tannin accumulation, and more
588 altered chloroplasts (with accumulation of abundant lipid-protein bodies). On the
589 contrary, much less evident changes were observed in RP, with FC and PO being
590 intermediate. The damage to chloroplast functionality has led to reduced
591 photosynthesis (Table 3). Investment in defence may, on the other hand, reduce
592 carbon availability for plant growth.

593 Compared to control, changes in leaf gas exchange, chlorophyll *a* fluorescence
594 and carboxylation parameters by E-O_3 showed similar responses in all species, as
595 indicated by no significant interactions between O_3 and species. Ozone induced
596 significant declines in A_{sat} and in chlorophyll *a* fluorescence parameters (ϕ_{PSII} and qP).
597 This decline in photosynthetic CO_2 assimilation was associated with significant
598 reductions in Vc_{max} and J_{max}, suggesting that biochemical limitations play an early and
599 primary role in the decline of CO_2 assimilation by O_3 (e.g., Calatayud et al., 2010;
600 Feng et al., 2011b; Cho et al., 2011). Changes in fluorescence parameters under
601 steady-state illumination may reflect a down-regulation process for adjusting the
602 production of reductive power and chemical energy to a lower demand by the
603 Calvin-Benson cycle (Calatayud et al., 2007). In a complementary study conducted
604 with the same plants but restricted to only three of the species (AA, FC and PO), E-O_3
605 increased stomatal sluggishness (i.e. slowed stomatal response) with FC and PO being
606 the most and less affected species, respectively (Hoshika et al., 2014). Increased
607 sluggishness may be related to accelerated leaf senescence in the cell physiological
608 processes (Paoletti et al., 2009), although the underlying mechanisms are still under
609 investigation (Hoshika et al., 2014). In the present study, chloroplasts of the guard

610 cells are sometimes altered, which could partly impair the normal performance of
611 these cells.
612 E-O_3 significantly increased total and reduced AsA contents in the leaves.
613 Activation of the AsA synthesis is a defence response against oxidative stress, as AsA
614 is a central metabolite in plant antioxidant system. It serves as a chemical scavenger
615 to protect plants by reducing free radicals, and also as a substrate of extracellular
616 enzymes such as the ascorbate peroxidase (APX) which detoxify peroxides; therefore
617 propagation of oxidative signaling diminishes (Burkey et al., 2006; Dizengremel et al.,
618 2013). Besides, all species in the present study showed an increase in phenolics
619 contents. Similar results have been previously reported in other tree species (Oksanen
620 et al., 2013). Phenolic metabolites probably increase O_3 tolerance of plants due to its
621 effectiveness as radicals and ROS scavengers (Grace, 2005; Langebartels et al., 2002).
622 Increased TAC levels are consistent with increased phenolics content as phenolic
623 compounds have been found to be the major contributors to the antioxidant properties
624 in extracts of different parts of 30 plants (e.g. Dudonné et al., 2009). In the present
625 study, however, all four species showed a similar response to O_3 in antioxidant levels.
626 Besides the increases in AsA, phenols or TAC, the different species were not able to
627 counteract photosynthesis impairment, cellular and tissue damage, and visible injury,
628 suggesting that the possible contribution of these physiological responses was
629 insufficient to offset the high levels of oxidative stress.
630 Considering visible injury, anatomical and ultrastructural responses, AA is the
631 most sensitive of all species as it developed symptoms the earliest and the percentage
632 of injuried leaves was the highest from the beginning. Anatomical and ultrastructural
633 alterations were also the severest in this species. On the other side, any of the RP
634 plants reached the higher injury classes, and visible injury was much less conspicuous
635 than the other species, with anatomical and ultrastructural changes being also
636 moderate. FC and PO were intermediate, with some of the leaves strongly affected by
637 a marked yellow or brown stippling. Several studies have shown that LMA is well
638 correlated with O_3 sensitivity of the species: plants with higher LMA are, in general,

639 more O_3 tolerant, partly due to the fact that they have a higher chlorophyll and
640 nitrogen content per area unit, supporting a more efficient photosynthesis activity,
641 which can better feed detoxification processes (Bussotti, 2008; Zhang et al., 2012).
642 Our results are not in line with such a hypothesis, probably because the investigated
643 species have a narrow LMA range (5.0-9.1 mg cm^{-2}). LMA is better related with O_3
644 tolerance when a larger range among species is considered (e.g., comparing deciduous
645 with evergreen species, Calatayud et al., 2011). The higher sensitivity in AA can
646 rather be explained as a combination of factors including a thinner palisade
647 parenchyma layer, less active antioxidant responses to O_3, and the highest g_s. The
648 palisade parenchyma is the most photosynthetically active tissue, so a reduced
649 thickness may imply that less apoplast surface is available for defense reactions
650 (Dizengremel *et al.*, 2013). The less active antioxidant responses in combination with
651 higher g_s (related to a higher O_3 uptake), would make this species more prone to
652 oxidative imbalances. These features are consistent with the pioneering, fast-growing
653 strategy of this species. On the other hand, although RP is also a sensitive species, its
654 lower g_s and, probably also, its stronger antioxidant responses could better withstand
655 O_3 stress, besides the fact of having lower constitutive antioxidant levels. Besides
656 showing more or less marked macro- and microscopic responses, it is noteworthy that
657 photosynthesis was also impaired in all the species, with CO_2 assimilation being
658 reduced. On the long run, such reductions are expected to affect CO_2 fixation as plant
659 biomass, one of the services of urban forests. In the present study, however, only one
660 growing season was covered and the effects on biomass were negligible (data not
661 shown).
662
663 **5. Conclusions**
664 The investigated four species are sensitive to O_3, as indicated by an increase in foliar
665 damage, accumulation of phenolic compounds in the leaf tissues, degradation of the
666 cell walls and organelles such as the chloroplasts, changes in antioxidant levels and
667 reduced photosynthesis rate. These changes might also alter plant interactions with

668 other abiotic and biotic stresses (Karnosky et al., 2005; Bussotti et al., 2008). The
669 current study suggests that sensitivity to O_3 should be taken into account for urban
670 tree plantations in areas at risk of high ozone concentrations, avoiding very sensitive
671 species such as AA. This is especially relevant for urban forests and large tree
672 plantations in parks or in green belts around cities rather than for trees planted in
673 streets, where O_3 is locally scavenged by reacting with NO traffic emissions. Further
674 studies of O_3 exposure under controlled or semi-controlled conditions involving many
675 urban trees are still needed in order to support decision making for tree plantation in
676 ozone polluted cities of China. Other additional factors to be considered in urban
677 greening species in relation to air pollution are their rate of BVOC emission and
678 capacity to remove O_3 and particulate matter (Paoletti et al., 2009; Calfapietra et al.,
679 2013).
680

681 **Acknowledgements**

682 This study has been funded by the Hundred Talents Program, Chinese Academy of
683 Sciences and State Key Laboratory of Urban and Regional Ecology. Collaboration
684 between RCEES and Fundación CEAM has been possible thanks to project AMIS
685 (Fate and Impact of Atmospheric Pollutants, PIRSES-GA-2011-295132), and by the
686 Chinese Academy of Sciences Visiting Professorships for Senior International
687 Scientists (Grant Number: 2013T2Z0009). VC also acknowledges the support of
688 PROMETEOII/2014/038 project (Generalitat Valenciana, G.V.), and FGB and JRA
689 that of PROMETEOII2013/021 (G.V.), and CGL2012-40058-C02-01/02 (MINECO).
690 We thank Mr. Yulong Zhang for the experimental management.
691

692 **6. References**

693 Ainsworth, E.A., Gillespie, K.M., 2007. Estimation of total phenolic content and other
694 oxidation substrates in plant tissues using Folin-Ciocalteu reagent. Nature Protocols
695 2, 875-877.

696 Benzie, I.F.F, Strain, J.J., 1996. The ferric reducing ability of plasma (FRAP) as a
697 measure of ‘antioxidant power’: the FRAP assay. Analytical Biochemistry 239,
698 70-76.

699 Burkey, K.O., Neufeld, H.S., Souza, L., Chappelka, A.H., Davison, A.W., 2006.
700 Seasonal profiles of leaf ascorbic acid content and redox state in ozone-sensitive
701 wildflowers. Environmental Pollution 143, 427-434.

702 Bussotti, F. 2008. Functional leaf traits, plant communities and acclimation processes
703 in relation to oxidative stress in trees: a critical overview. Global Change Biology
704 14, 2727–2739.

705 Bussotti, F., Agati, G., Desotgiu, R., Matteini, P., Tani, C., 2005. Ozone foliar
706 symptoms in woody plant species assessed with ultrastructural and fluorescence
707 analysis. New Phytologist 166, 941–955.

708 Calatayud V., Cerveró J., Sanz M.J., 2007. Foliar, physiologial and growth responses
709 of four maple species exposed to ozone. Water, Air, and Soil Pollution 185,
710 239-254.

711 Calatayud V., Marco F., Cerveró J., Sánchez-Peña G., Sanz M.J., 2010. Contrasting
712 ozone sensitivity in related evergreen and deciduous shrubs. Environment Pollution
713 158, 3580-3587.

714 Calatayud,V., García-Breijo, F.J, Cervero, J., Reig-Armiñana, J., Sanz, M.J., 2011.
715 Physiological, anatomical and biomass partitioning responses to ozone in the
716 Mediterranean endemic plant *Lamottea dianae*. Ecotoxicology and Environmental
717 Safety 74,1131-1138.

718 Calfapietra, C., Fares, S., Manes, F., Morani, A., Sgrigna, G., Loreto, F., 2013. Role of
719 biogenic volatile organic compounds（BVOC）emitted by urban trees on ozone
720 concentration in cities: a review. Environmental Pollution 183,71-80.

721 Chen, W., Tang, H.Z., Zhao, H.M., 2015. Diurnal, weekly and monthly spatial
722 variations of air pollutants and air quality of Beijing. Atmospheric Environment
723 119, 21-34.

724 Cho K., Tiwari S., Agrawal S., Torres N., Agrawal M., Sarkar A., et al., 2011.
725 Tropospheric ozone and plants: absorption, responses, and consequences, in:

726 Whitacre D.W. (Eds.), Reviews of Environmental Contamination and Toxicology
727 Volume 212. Springer, PP. 61-111.

728 Dizengremel, P., Jolivet, Y., Tuzet, A. Ranieri, A., Le Thiec, D., 2013. Integrative
729 leaf-level ozone phytotoxic ozone dose assessment for forest risk modeling, in:
730 Matyssek, R., Clarke, N., Cudlin, P., Mikkelsen T.N., Tuovinen, J.P., Wieser, G.,
731 Paoletti, E., (Eds.), Climate Change, Air Pollution and Global Challenges.
732 Developments in Environmental Sciences 13. Elsevier, Netherlands, pp. 267-288.

733 Dudonne, S., Vitrac, X., Coutiere, P., Woillez, M., Mérillon, J.M., 2009. Comparative
734 study of antioxidant properties and total phenolic content of 30 plant extracts of
735 industrial interest using DPPH, ABTS, FRAP, SOD, and ORAC assays. Journal of
736 Agricultural and Food Chemistry 57, 1768-1774.

737 Feng, Z.Z., Hu, E.Z.,Wang, X.K., Jiang, L.J., Liu, X.J., 2015a. Ground-Level O_3
738 pollution and its impacts on food crops in China: a review. Environmental Pollution
739 199, 42-48.

740 Feng, Z.Z., Liu, X.J., Zhang, F.S., 2015b. Air pollution affects food security in China:
741 taking ozone as an example. Frontier Agricultural. Sciences and Engineer 2(2),
742 152-158.

743 Feng, Z.Z., Niu, J.F., Zhang, W.W., Wang, X.K., Yao, F.F., Tian, Y., 2011a. Effects of
744 ozone exposure on Sub-Tropical evergreen *Cinnamomum Camphora* seedlings
745 grown in different nitrogen loads. Trees 25, 617-625.

746 Feng, Z.Z., Pang, J., Kobayashi, K., Zhu, J., Ort, D.R., 2011b. Differential responses
747 in two varieties of winter wheat to elevated ozone concentration under fully
748 open-air field conditions. Global Change Biology 17, 580-591.

749 Feng, Z.Z., Sun, J.S., Wan,W.X., Hu, E.Z., Calatayud, V., 2014. Evidence of
750 widespread ozone-induced visible injury on plants in Beijing, China.
751 Environmental Pollution 193, 296-301.

752 Gao, J.C., Guo, G.J., Guo, Y.M., Wang, X.X., Du, Y.C., 2011. Measuring plant leaf
753 area by scanner and ImageJ software. China Vegetables 2, 73-77.

García-Breijo, F.J., Reig-Armiñana, J., Bautista-Peris, B., Calatayud, V., Cerveró, J., Sanz, M.J., 2008. Effets anatomiques de l'ozone sur le térébinthe (*Pistacia terebinthus*). Forêt Méditerranéenne 29, 13–22.

Gillespie, K.M., Ainsworth, E.A., 2007. Measurement of reduced, oxidized and total ascorbate content in plants. Nature Protocols 2, 871-874.

Grace, S.C., 2005. Phenolics as antioxidants. In: Smirnoff, N. (Eds.), Antioxidants and Reactive Oxygen Species in Plants. Blackwell Publishing Ltd, Oxford, UK, pp. 141–168.

Grantz, D., 2003. Ozone impacts on cotton: Towards an integrated mechanism. Environmental Pollution 126, 331-344.

Gravano, E., Giulietti, V., Desotgiu, R., Bussotti, F., Grossoni, P., Gerosa, G., et al., 2003. Foliar response of an *Ailanthus altissima* clone in two sites with different levels of ozone-pollution. Environmental Pollution 121, 137–146.

Günthardt-Goerg, M.S.,Vollenweider, P., 2007. Linking stress with macroscopic and microscopic leaf response in trees: New diagnostic perspectives. Environmental Pollution 147, 467-488.

Harris, J.B., Schaefer, V.G., 1981. Some correlated events in aging leaf tissues of tree, tomato and tobacco. Botanical Gazette, 43-54.

Hoshika, Y., Carriero, G., Feng, Z., Zhang, Y., Paoletti, E., 2014. Determinants of stomatal sluggishness in ozone-exposed deciduous tree species. Science of the Total Environment 481, 453-458.

IPCC, 2013. Intergovernmental Panel on Climate Change. Fifth Assessment Report. http://www.ipcc.ch/report/ar5/index.shtml.

Kangasjärvi, J., Talvinen, J., Utriainen, M., Karjalainen, R., 1994. Plant defense systems induced by ozone: commissioned review. Plant Cell & Environment 17, 783–794.

Karnosky D., Pregitzer K. S., Zak D. R., Kubiske M. E., Hendrey G., Weinstein D., Nosal M., Percy, K.E., 2005. Scaling ozone responses of forest trees to the ecosystem level in a changing climate. Plant, Cell and Environment, 965–981.

783 Kivimäenpää, M., Sutinen, S., Calatayud, V., Sanz, M.J., 2010. Visible and
784 microscopic needle alterations of mature Aleppo Pine (*Pinus halepensis*) trees
785 growing on an ozone gradient in eastern Spain. Tree Physiology 30, 541-554.

786 Krupa, S., McGrath, M.T., Andersen, C.P., Booker, F., Burkey, K.O., Chappelka, A.H.,
787 et al., 2000. Ambient ozone and plant health. Plant Disease 85, 4-12.

788 Landolt, W., Günthardt-Goerg, M.S., Pfenninger, I., Einig, W., Hampp, R., Maurer, S.,
789 et al., 1997. Effect of fertilization on ozone-induced changes in the metabolism of
790 birch (*Betula pendula*) leaves. New Phytologist 137, 389–397.

791 Langebartels, C., Schraudner, M., Heller, W., Ernst, D., Sandermann, H., 2002.
792 Oxidative stress and defense reactions in plants exposed to air pollutants and UV-B
793 radiation, In: Inze´, D., Van Montagu, M. (Eds.), Oxidative Stress in Plants.Taylor
794 & Francis, London, UK, pp.105–135.

795 Lee, J.B., Cha, J.S., Hong, S.C., Choi, J.Y., Myoung, J.S., Park, R.J., et al., 2015.
796 Projections of summertime ozone concentration over East Asia under multiple
797 IPCC SRES emission scenarios. Atmospheric Environment 106, 335-346.

798 Lichtenthaler, H.K., 1987. Chlorophylls and carotenoids: pigments of photosynthetic
799 biomembranes. Methods in Enzymology 148, 350-382.

800 LRTAP Convention, 2010. Manual on Methodologies and Criteria for Modelling and
801 Mapping Critical Loads & Levels and Air Pollution Effects, Risks and Trends. In:
802 Chapter 3: Mapping Critical Levels for Vegetation.

803 Matile, P., 1992.Chloroplast senescence. In: Baker, N.R., Thomas H. (Eds.), Crop
804 Photosynthesis: Spatial and Temporal Determinants. Elsevier Ltd., pp. 413-440.

805 Matyssek, R., Bytnerowicz, A., Karlsson, P.E., Paoletti, E., Sanz, M., Schaub, M., et
806 al. 2007. Promoting the O_3 flux concept for European forest trees. Environmental
807 Pollution, 146, 587–607.

808 Matyssek, R., Günthardt-Goerg, M.S., Saurer, M., Keller, T., 1992. Seasonal growth,
809 $\delta^{13}C$ in leaves and stem, and phloem structure of birch (*Betula pendula*) under low
810 ozone concentrations. Trees 6, 69–76.

811 Nowak, D,J., Hirabayashi, S., Bodine, A., Greenfield, E.G, 2014. Tree and forest
812 effects on air quality and human health in the United States. Environmental
813 Pollution 193, 119-129.

814 Oksanen, E., Keski-Saari, S., Kontunen-Soppela, S., Keinänen, M., 2013.
815 Metabolomics and transcriptomics increase our understanding about defence
816 responses and genotypic differences of northern deciduous trees to elevating ozone,
817 CO_2 and climate warming. Climate Change, Air Pollution and Global Challenges .
818 Developments in Environmental Science 13, 309-326.

819 Paoletti, E., Contran, N., Bernasconi, P., Günthardt-Goerg, M.S.,Vollenweider, P.,
820 2009. Structural and physiological responses to ozone in Manna ash (*Fraxinus*
821 *Ornus* L.) leaves of seedlings and mature trees under controlled and ambient
822 conditions. Science of the Total Environment 407, 1631-1643.

823 Paoletti, E., Ranieri, A., Lauteri, M. 2008. Moving toward effective ozone flux
824 assessment. Environmental Pollution, 156, 16–19.

825 Rao, M.V., Koch, J.R.,Davis, K.R., 2000. Ozone: A Tool for Probing Programmed
826 Cell Death in Plants, In: Lam E., Fukuda H., Greenberg J. (Eds.), Programmed Cell
827 Death in Higher Plants. Springer, pp.101-114.

828 Reig-Armiñana, J., Calatayud, V., Cerveró, J., Garcıa-Breijo, F., Ibars, A.,Sanz, M.,
829 2004. Effects of ozone on the foliar histology of the mastic plant (*Pistacia*
830 *Lentiscus* L.). Environmental Pollution 132, 321-331.

831 Sandermann, H., Ernst, D., Heller, W., Langebartels, C., 1998. Ozone: An abiotic
832 elicitor of plant defence reactions. Trends in Plant Science 3, 47-50.

833 Sharkey, T.D., Bernacchi, C.J., Farquhar, G.D., Singsaas, E.L., 2007. Fitting
834 photosynthetic carbon dioxide response curves for C3 leaves. Plant, Cell &
835 Environment 30, 1035-1040.

836 Stone, B.A., Clarke, A.E. ,1992. Chemistry and biology of 1, 3-[beta]-glucans. La
837 Trobe University Press Melbourne.

838 The Royal Society, 2008. Ground-level ozone in the 21st century: future trends,
839 impacts and policy implications. Science Policy Report 15/08. The Royal Society,
840 London.

841 Valkama, E., Koricheva, J., Oksanen, E., 2007. Effects of elevated O_3, alone and in
842 combination with elevated CO_2, on tree leaf chemistry and insect herbivore
843 performance: a meta-analysis. Global Change Biology 13, 184–201.

844 Vingarzan, R., 2004. A review of surface ozone background levels and trends.
845 Atmospheric Environment 38, 3431-3442.

846 Vollenweider, P., Ottiger, M.,Günthardt-Goerg, M., 2003. Validation of leaf ozone
847 symptoms in natural vegetation using microscopical methods. Environmental
848 Pollution 124, 101-118.

849 Wang, X.P., Mauzerall, D.L., 2004. Characterizing distributions of surface ozone and
850 its impact on grain production in China, Japan and south Korea: 1990 and 2020.
851 Atmospheric Environment 38, 4383-4402.

852 Yamaji, K., Ohara, T., Uno, I., Kurokawa, J.I., Pochanart, P.,Akimoto, H., 2008.
853 Future prediction of surface ozone over east Asia using models-3 community
854 multiscale air quality modeling system and regional emission inventory in Asia.
855 Journal of Geophysical Research -Atmospheres 113, 2156-2202.

856 Yang, J., McBride, J., Zhou, J.X., Sun, Z.Y., 2005. The urban forest in Beijing and its
857 role in air pollution reduction. Urban Forestry & Urban Greening 3, 65-78.

858 Yuan, X.Y., Calatayud, V., Jiang, L.J., Manning, W.J., Hayes, F., Tian, Y., Feng, Z.Z.,
859 2015. Assessing the effects of ambient ozone in China on snap bean genotypes by
860 using ethylenediurea (EDU). Environmental Pollution 205, 199-208.

861 Zhang, W.W., Feng, Z.Z., Wang, X.K., Niu, J.F., 2012. Responses of native
862 broadleaved woody species to elevated ozone in subtropical China. Environmental
863 Pollution 163, 149-157.